Adv. Sci. Res., 13, 107–112, 2016
www.adv-sci-res.net/13/107/2016/
doi:10.5194/asr-13-107-2016

Advances in Science & Research
Open Access Proceedings

Influence of sea surface roughness length parameterization on Mistral and Tramontane simulations

Anika Obermann, Benedikt Edelmann, and Bodo Ahrens

Institut für Atmosphäre und Umwelt, Goethe Universiät Frankfurt, Altenhöferallee 1, 60438 Frankfurt am Main, Germany

Correspondence to: Anika Obermann (obermann@iau.uni-frankfurt.de)

Received: 12 January 2016 – Revised: 21 June 2016 – Accepted: 21 June 2016 – Published: 8 July 2016

Abstract. The Mistral and Tramontane are mesoscale winds in southern France and above the Western Mediterranean Sea. They are phenomena well suited for studying channeling effects as well as atmosphere–land/ocean processes. This sensitivity study deals with the influence of the sea surface roughness length parameterizations on simulated Mistral and Tramontane wind speed and wind direction. Several simulations with the regional climate model COSMO-CLM were performed for the year 2005 with varying values for the Charnock parameter α. Above the western Mediterranean area, the simulated wind speed and wind direction pattern on Mistral days changes depending on the parameterization used. Higher values of α lead to lower simulated wind speeds. In areas, where the simulated wind speed does not change much, a counterclockwise rotation of the simulated wind direction is observed.

1 Introduction

The Mistral and Tramontane are winds in southern France, which are channeled by the Rhône and Aude valleys before blowing over the Mediterranean Sea. Since this winds are caused by similar synoptic situations, they often occur at the same time (Georgelin et al., 1994; Guenard et al., 2005). They play a crucial role for deep water formation in the Gulf of Lion and for the understanding of the Mediterranean Sea circulation (Schott et al., 1996; Béranger et al., 2010). On Mistral and Tramontane days, simulations with the regional climate model COSMO-CLM (CCLM) with 0.088° grid spacing were found to be able to simulate Mistral and Tramontane wind patterns slightly overestimating 10 m wind speed compared to satellite and buoy observations (Obermann et al., 2016).

This sensitivity study investigates the influence of the sea surface roughness length parameterization on the patterns of Mistral and Tramontane wind speeds and wind directions above the Mediterranean Sea in CCLM simulations. The aim of this study is not to find a better parameterization of surface roughness, but a discussion of the sensititvity of wind patterns of an atmospheric model on its parameterization. A complete description of the ocean-atmosphere interaction and, therefore, the sea surface roughness, also should account for ocean currents, waves, and interaction between these phenomena (Carniel et al., 2016; Ricchi et al., 2016).

Three atmosphere only simulation runs with different parameterizations were performed for the year 2005 in which Mistral occurred at 88 days. 81 of which in coincidence with Tramontane (Edelmann, 2015). The Mistral and Tramontane days in 2005 were identified using 13 observation stations in Southern France which provided gust information along the dominant Mistral and Tramontane directions. An explanation of the full algorithm to identify Mistral and Tramontane days can be found in Obermann et al. (2016).

2 Regional climate simulations

The CCLM model (Rockel et al., 2008; Kothe et al., 2014) is the climate version of the nonhydrostatic atmospheric COSMO model, which is used by the German Weather Service for operational weather forecasts. It consists of the primitive thermo-hydrodynamical equations for a fully compressible flow in moist atmosphere formulated in rotated geographical coordinates and generalized terrain following height coordinates. The simulations of this study were performed by Goethe Universität Frankfurt (GUF) using the

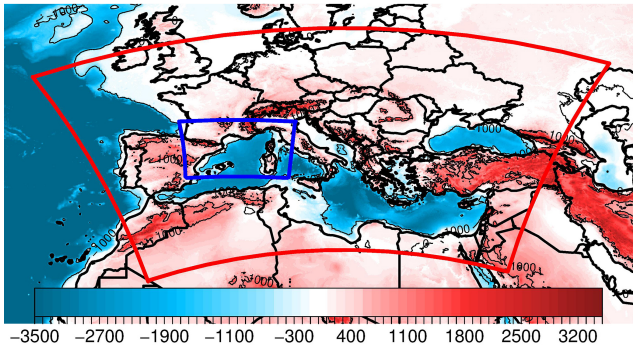

Figure 1. ETOPO1 (Amante and Eakins, 2009) orography and bathymetry data interpolated onto a 0.088° grid [m]. MedCORDEX domain in red, nested domain in blue.

model version CCLM 5-0-2 with a turbulent kinetic energy (TKE) transfer scheme for surface fluxes and the soil model TERRA. A two time-level second-order Runge–Kutta scheme was used. Spectral nudging, condensation, convection and grid scale precipitation were enabled (Edelmann, 2015).

2.1 Nesting strategy

The simulations cover a domain of $1140 \times 800\,\mathrm{km}^2$ encompassing Southern France and a large part of the western Mediterranean Sea (area marked in blue in Fig. 1). The simulations are nested into a CCLM simulation (model version CCLM 4-8-18) on the larger MedCORDEX domain which covers the Mediterranean Sea, the Black Sea, and the surrounding land areas (Ruti et al., 2015, area marked in red in Fig. 1). The simulation on the outer domain was initialized on 1 January 1989, while the simulations on the inner domain cover 1 year, starting from 1 January 2005. Horizontal grid spacing for both domains is 0.088° with 40 vertical levels and a time step of 30 s. One way nesting with three boundary lines (i.e. about 30 km) is used. The boundary data are updated every three hours and interim time steps are linearly interpolated (Edelmann, 2015).

2.2 Forcing data

The forcing data for the simulation on the MedCORDEX domain comes from ERA-Interim (Dee et al., 2011). The information on sea surface temperature (SST) is provided as daily means and linearily interpolated to the CCLM grid.

2.3 Variation of roughness length

The roughness length z_0 depends on the properties of ocean waves and, therefore, on wind speeds over the sea surface. A classical parameterization of sea surface roughness was introduced by Charnock (1955):

$$z_0 = \frac{\alpha}{g} \times u_*^2. \tag{1}$$

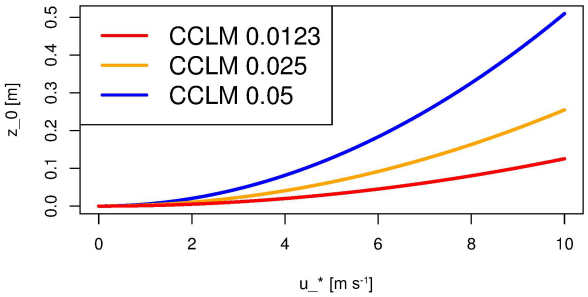

Figure 2. Roughness length as function of u_* for three values of Charnock parameter α.

The parameterization of sea surface roughness varies between regional climate models. For example, the Weather Research and Forecasting (WRF) model (Colin et al., 2010) uses $\alpha = 0.0185$ and adds a constant of 1.59×10^{-5} m to avoid zero roughness length. Alternative versions of the Charnock formula from five regional climate models have been tested in CCLM. A detailed discussion of these parameterizations and comparison to observational data can be found in Edelmann (2015). In this study, the focus is on the variation of the CCLM parameterization of the Charnock formula. In CCLM (Doms et al., 2011), the Charnock formula is implemented as

$$z_0 = \frac{\alpha}{g} \times \max\left(u_*^2, w_*^2\right). \tag{2}$$

Here, α denotes the Charnock parameter, g the gravity constant, u_* the friction velocity, and w_* the free convection scaling velocity. In the standard configuration, CCLM uses a value of $\alpha = 0.0123$. In this study, two larger values of the Charnock parameter ($\alpha = 0.025$ and $\alpha = 0.05$) have been tested because of the aforementioned overestimation of wind speed in CCLM 0.088° simulations. Even though large values of α do not have a physical background, they give the possibility to test the sensitivity of wind patterns on α. Figure 2 shows the roughness length as function of u_* for the three values of α tested in this study. All other parameters and the forcing data are the same for all three simulation runs.

3 Results

3.1 Reference simulation

Figure 3a shows the mean sea level pressure during the Mistral days in 2005 from the reference simulation ($\alpha = 0.123$). The situation is characterized by a pressure low visible close to Corsica in the right part of the figure. Figure 3b shows the mean 10 m wind speeds during the same days. The highest

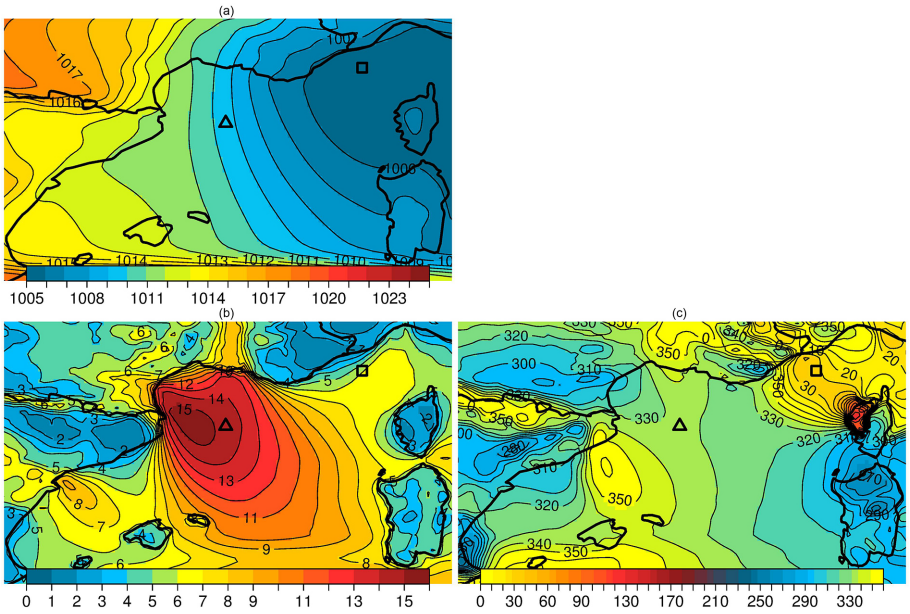

Figure 3. Mean sea level pressure [hPa] **(a)**, mean 10 m wind speed [$m\,s^{-1}$] **(b)** and mean 10 m wind direction [°] **(c)** during Mistral events in the reference simulation ($\alpha = 0.0123$) in the Gulf of Lion area. Locations of Lion (triangle) and Azur (square) buoys.

wind speeds occur over the Mediterranean Sea in the Gulf of Lions. The effect of channeling (i.e. the acceleration of wind in valleys) is visible in the Rhône and Aude valleys. Two more local wind phenomena are visible during Mistral days: in the Ebro valley south of the Pyrennes, the local wind Cierzo causes wind speeds up to 9 $m\,s^{-1}$ during Mistral days. The Italian Tramontane between Alps and Apennines reaches up to 5 $m\,s^{-1}$. During Mistral and Tramontane events, the mean wind direction is north to northwest (Fig. 3c). In the Rhône valley, Mistral comes mainly from north, while the dominant Tramontane direction in the Aude valley is west-northwest.

3.2 Changes in wind speed and direction along the variation of α

Figure 4 shows the bias of the simulation runs with $\alpha = 0.025$ and $\alpha = 0.05$ compared to the reference run ($\alpha = 0.0123$). A decrease in wind speeds is observed for increasing α (Fig. 4a, c) in large parts of the modeling domain. The strongest decrease in wind speed for increasing α occurs in areas with high absolute wind speeds in the reference run (Fig. 3b).

With increasing α, the wind direction changes to a more counterclockwise rotated direction south of the Balearic Islands, between the Alps and Corsica, as well as from Corsica to the northern Apennines (Fig. 4c, d). In the residual areas around Corsica and at the coast close to Alps and Pyrenees, the wind is rotated clockwise. The variation of α exerts only a weak influence upon the sea level pressure field: on one hand the sea level pressures undergo only slight changes in general. On the other hand the position of the minimum sea level pressure within the domain does not move (not shown).

3.3 Buoy observations

In the area of interest, two stationary buoys measure wind speed and wind direction (and further parameters) several times a day. The Lion buoy is located in the Gulf of Lion (42.1° N, 4.7° E), the Azur buoy is located close to the French-Italian border (43.4° N, 7.8° E). The buoy locations are marked in Figs. 3 and 4. Figure 5 shows wind speed density plots for both buoy locations. The wind speed is overestimated by all three simulations, with the reference ($\alpha = 0.0123$) having the largest bias.

As can be seen from Fig. 3c, the wind comes from a north-westerly direction at the Lion buoy location during Mistral days. The simulations show a small clockwise rotated bias at this location. The main wind direction for the Azur buoy location is north-easterly. Here, the simulations show a counter-clockwise rotated bias. As can be seen from Fig. 4c and d, the wind direction differences between the three simulations at both buoy locations are small.

3.4 Interconnection of wind speed and wind direction change

The Mistral events in 2005 are divided in two groups, depending on the observed wind speed at the Lion buoy. 32 days showed daily mean 10 m winds below 12 $m\,s^{-1}$, 52 showed wind speeds above 12 $m\,s^{-1}$. For the remaining 4 days no observations were available. For both the

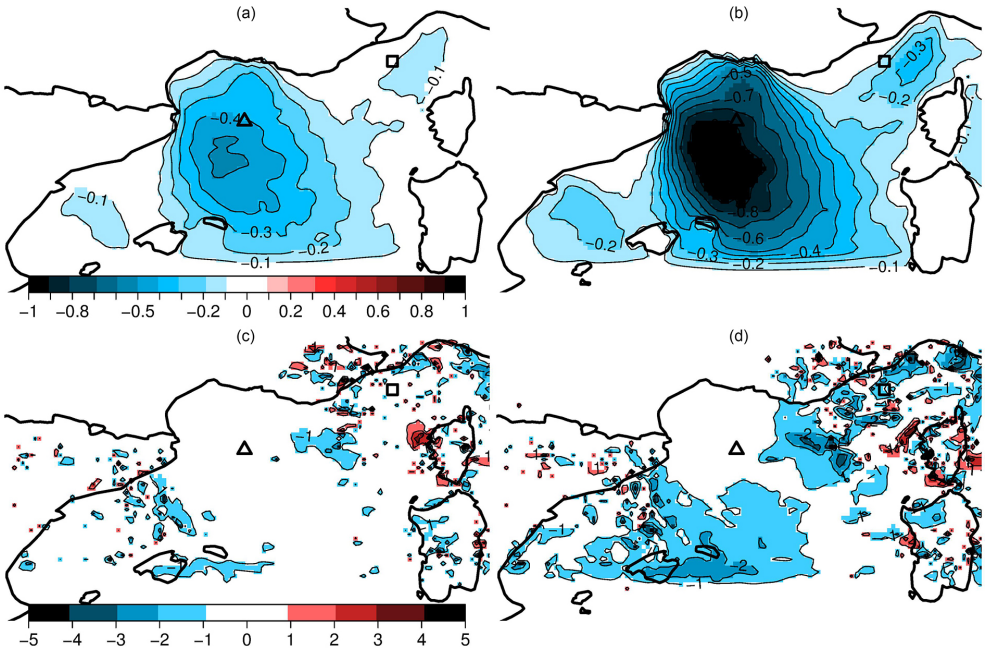

Figure 4. 10 m wind speed bias [$\mathrm{m\,s^{-1}}$] **(a, b)** and 10 m wind direction bias [°] **(c, d)** for $\alpha = 0.025$ **(a, c)** and $\alpha = 0.05$ **(b, d)** with respect to reference ($\alpha = 0.0123$). Locations of Lion (triangle) and Azur (square) buoys.

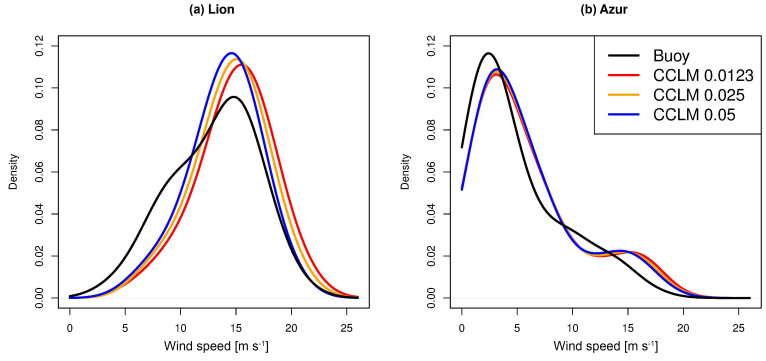

Figure 5. 10 m wind speed density distribution at Gulf of Lion buoy location **(a)** and Azur buoy location **(b)**.

$\alpha = 0.025$ and the $\alpha = 0.05$ run, the wind speed decreased stronger on days with high wind speeds in the reference run. On days with lower wind speeds, the change in direction is stronger than for days with high wind speeds (not shown).

3.5 Influence of sea surface temperature

The daily mean sea surface temperature (SST) in the area 3–8° E and 38.5–43.5° N is used to divide the Mistral days in days with high SSTs (above 20 °C) and days with low SSTs (below 14 °C). 29 Mistral days of 2005 are in each of the groups. When calculating the biases as shown in Fig. 4, the influence of SST on wind speed and direction changes can be derived. The wind speed change compared to the reference is stronger during cold Mistral events, while the wind direction changes are more pronounced during warm events. The relative change in wind speed is of the same magnitude during cold and warm events, due to the stronger wind speeds during cold events (not shown).

4 Discussion

The 10 m wind speed decreases in large parts of the modeling domain for increasing α as expected from the u_*^2-dependence of Eq. (2). This result is in agreement with the findings of Thévenot et al. (2015), who showed that an increase in wave height (and a resulting increase in z_0) leads to lower wind speeds.

The largest differences are found for the Gulf of Lion, where the highest wind speeds are observed in the reference simulation. Another effect occurs in wind direction: here, the

bias is the largest in the area between the Alps and Corsica (that is, in the north-eastern part of the investigation domain) where only minor wind speed changes are observed. From the wind speed dependence of the Coriolis force one would expect that slower winds (as they are observed for higher values of α) come from a more counterclockwise rotated direction. Consequently, this effect should be stronger where the wind speed change is larger, but this is not present in the simulations.

Indeed, the change of wind speed and wind direction do not occur at the same time and location. The patterns found in this sensitivity study could be due to several phenomena. The counterclockwise rotation at the borders of the main flow could be due to the flow becoming more agestrophic with decreasing wind speed. Coriolis force decreases with decreasing wind speeds, and the counteracting pressure gradient force could cause the rotation. Giles (1977) discussed the Coanda effect resulting in the Mistral staying attached to the Alps. This counteracts the clockwise rotation of Mistral and Tramontane due to the Coriolis force. The increased α values could potentially result in a broadened Mistral and Tramontane flow, which would extend further to the east. A consequence of which would be a smaller bias in wind speed and a counter-clockwise rotated wind between Alps and Corsica. The situation east of Corsica could be similar in the case of the Italian Tramontane.

On days with higher SSTs, the wind direction changes are stronger than on days with low SSTs, while the wind speed changes are larger on days with low SSTs. An increased α parameter influences the winter and spring Mistral days (i.e., days with low SSTs) more in terms of wind speed, while the influence on wind direction is the strongest during summer and autumn (i.e. days with high SSTs).

5 Conclusions

Three values for the Charnock parameter α have been tested within the regional climate model COSMO-CLM. In the Western Mediterranean area, the wind pattern on Mistral days changes depending on the parameterization used. While the whole sea level pressure pattern does not change much, higher values of α lead to lower wind speeds in the main flow. The overestimation of wind speeds found in the reference simulation was reduced. A counterclockwise rotation of the wind on the left hand border of the flow is observed for higher valutes of α. This could be due to a change in the balance between the wind speed dependent Coriolis force and pressure gradient force as well as corner effects as the so called Coanda effect, which causes a flow to stay close to nearby mountain ranges. Further studies are needed to test these assumptions and to study the sensitivity to roughness length changes due to other phenomena (e.g., ocean currents and waves).

6 Data availability

The run scripts and simulation data are archived at the Goethe University Frankfurt. The CCLM code is available from the CLM Community website http://www.clm-community.eu.

Author contributions. Benedikt Edelmann carried out the experimental simulations. Anika Obermann prepared the figures and the manuscript with contributions from all co-authors.

Acknowledgements. This work is part of the Med-CORDEX initiative (www.medcordex.eu) supported by the HyMeX programme (www.hymex.org). Gust time series were provided by Valérie Jacq, Météo-France. Buoy data were provided by Marie-Noelle Bouin and Guy Caniaux, Météo-France. Simulations were performed at DKRZ and LOEWE-CSC. We acknowledge support from the German Federal Ministry of Education and Research (BMBF) under grant MiKliP II (FKZ 01LP1518C). Bodo Ahrens acknowledges support from Senckenberg BiK-F. We thank two anonymous reviewers.

Edited by: M. M. Miglietta
Reviewed by: two anonymous referees

References

Amante, C. and Eakins, B.: ETOPO1 1 Arc-Minute Global Relief Model: Procedures, Data Sources and Analysis, NOAA Technical Memorandum NESDIS NGDC-24, doi:10.7289/V5C8276M, 2009.

Béranger, K., Drillet, Y., Houssais, M.-N., Testor, P., Bourdallé-Badie, R., Alhammoud, B., Bozec, A., Mortier, L., Bouruet-Aubertot, P., and Crépon, M.: Impact of the spatial distribution of the atmospheric forcing on water mass formation in the Mediterranean Sea, J. Geophys. Res., 115, C12041, doi:10.1029/2009JC005648, 2010.

Carniel, S., Benetazzo, A., Bonaldo, D., Falcieri, F. M., Miglietta, M. M., Ricchi, A., and Sclavo, M.: Scratching beneath the surface while coupling atmosphere, ocean and waves: Analysis of a dense water formation event, Ocean Model., 101, 101–112, doi:10.1016/j.ocemod.2016.03.007, 2016.

Charnock, H.: Wind stress on a water surface, Q. J. Roy. Meteor. Soc., 81, 639–640, doi:10.1002/qj.49708135027, 1955.

CLM-Community: CCLM code, available at: http://www.clm-community.eu, last access: 1 July 2016.

Colin, J., Déqué, M., Radu, R., and Somot, S.: Sensitivity study of heavy precipitation in Limited Area Model climate simulations: influence of the size of the domain and the use of the spectral nudging technique, Tellus A, 62, 591–604, doi:10.1111/j.1600-0870.2010.00467.x, 2010.

Dee, D. P., Uppala, S. M., Simmons, A. J., et al.: The ERA-Interim reanalysis: configuration and performance of the data assimilation system, Q. J. Roy. Meteor. Soc., 137, 553–597, doi:10.1002/qj.828, 2011.

Doms, G., J. Foerstner, E. H., Herzog, H.-J., Mironov, D., Raschendorfer, M., Reinhardt, T., Ritter, B., Schrodin, R., Schulz, J.-P., and Vogel, G.: A Description of the Nonhydrostatic Regional COSMO Model, Part II: Physical Parameterization, Consortium for Small-Scale Modelling, 161 pp., 2011.

Edelmann, B.: Dependence of COSMO-CLM simulated Wind on Wind Stress Parameterisation in the Gulf of Lion, Master's thesis, Goethe Universität Frankfurt, 2015.

Georgelin, M., Richard, E., Petitdidier, M., and Druilhet, A.: Impact of Subgrid-Scale Orography Parameterization on the Simulation of Orographic Flows, Mon. Weather Rev., 122, 1509–1522, doi:10.1175/1520-0493(1994)122<1509:IOSSOP>2.0.CO;2, 1994.

Giles, B.: Fluidics, the Coanda Effect, and some orographic winds, Archiv für Meteorologie, Geophysik und Bioklimatologie, Serie A, 25, 273–279, doi:10.1007/BF02321800, 1977.

Guenard, V., Drobinski, P., Caccia, J.-L., Campistron, B., and Bench, B.: An Observational Study of the Mesoscale Mistral Dynamics, Bound.-Lay. Meteorol., 115, 263–288, doi:10.1007/s10546-004-3406-z, 2005.

Kothe, S., Panitz, H.-J., and Ahrens, B.: Analysis of the radiation budget in regional climate simulations with COSMO-CLM for Africa, Meteorol. Z., 23, 123–141, doi:10.1127/0941-2948/2014/0527, 2014.

Obermann, A., Bastin, S., Belamari, S., Conte, D., Gaertner, M. A., Li, L., and Ahrens, B.: Mistral and Tramontane wind speed and wind direction patterns in regional climate simulations, Clim. Dynam., online first, doi:10.1007/s00382-016-3053-3, 2016.

Ricchi, A., Miglietta, M. M., Falco, P. P., Benetazzo, A., Bonaldo, D., Bergamasco, A., Sclavo, M., and Carniel, S.: On the use of a coupled ocean-atmosphere-wave model during an extreme cold air outbreak over the Adriatic Sea, Atmos. Res., 172–173, 48–65, doi:10.1016/j.atmosres.2015.12.023, 2016.

Rockel, B., Will, A., and Hense, A.: The regional climate model COSMO-CLM (CCLM), Meteorol. Z., 17, 347–348, 2008.

Ruti, P., Somot, S., Giorgi, F., et al.: MED-CORDEX initiative for Mediterranean Climate studies, B. Am. Meteorol. Soc., doi:10.1175/BAMS-D-14-00176.1, 2015.

Schott, F., Visbeck, M., Send, U., Fischer, J., Stramma, L., and Desaubies, Y.: Observations of deep convection in the Gulf of Lions, northern Mediterranean, during the winter of 1991/92, J. Phys. Oceanogr., 26, 505–524, 1996.

Thévenot, O., Bouin, M.-N., Ducrocq, V., Lebeaupin Brossier, C., Nuissier, O., Pianezze, J., and Duffourg, F.: Influence of the sea state on Mediterranean heavy precipitation: a case-study from HyMeX SOP1, Q. J. Roy. Meteor. Soc., doi:10.1002/qj.2660, online first, 2015.